

## NEW CONSTRAINTS ON SN IA PROGENITOR MODELS

KRZYSZTOF BELCZYNSKI<sup>1,2</sup>, TOMASZ BULIK<sup>3</sup>, ASHLEY J. RUITER<sup>1</sup><sup>1</sup> New Mexico State University, Dept. of Astronomy, 1320 Frenger Mall, Las Cruces, NM 88003<sup>2</sup> Tombaugh Fellow<sup>3</sup> Nicolaus Copernicus Astronomical Center, Bartycka 18, 00-716 Warszawa, Poland; kbelczyn@nmsu.edu, bulik@camk.edu.pl, aruiter@nmsu.edu*Draft version July 17, 2018*

## ABSTRACT

We use the **StarTrack** population synthesis code to discuss potential progenitor models of SN Ia: single degenerate scenario, semi-detached double white dwarf binary and double degenerate scenario. Using the most recent calculations of accretion onto white dwarfs, we consider SN Ia explosions of various white dwarfs in binary systems. We calculate the evolutionary delay times from the zero age main sequence to the explosion, and verify which scenarios can satisfy the constraints found by Strolger et al. (2004), i.e. a delay time of 2-4 Gyrs. It is found that the semi-detached double white dwarf binary model is inconsistent with observations. Only SN Ia progenitors in the double degenerate scenario are compatible with observations in all tested evolutionary models, with a characteristic delay time of  $\sim 3$  Gyrs. If double degenerate mergers are excluded as SN Ia progenitors, we find that the single degenerate scenario may explain the observed delay times for models with low common envelope efficiency. It is also noted that the delay time distributions within the various tested SN Ia scenarios vary significantly and potentially can be used as an additional constraint on progenitor models.

*Subject headings:* binaries: close — stars: evolution — stars: formation — supernovae: general

## 1. INTRODUCTION

Supernovae Ia are used as precise distance indicators, and the results of deep supernova searches (Schmidt et al. 1998; Perlmutter 1999; Riess et al. 2001; Tonry 2003) have led to the conclusion that the Universe expansion rate is accelerating. This along with the WMAP results (Tegmark et al. 2004) provide evidence that the matter density in the Universe is  $\Omega_M \approx 0.3$ , and that the cosmological constant density is  $\Omega_\Lambda \approx 0.7$ . These results depend crucially on the assumption that SN Ia are standard candles. This assumption could be tested if the origins of SN Ia are recognized. Therefore, any new observational and theoretical constraints on their progenitors are very useful.

The theoretical search for SN Ia progenitors is usually carried out with the population synthesis method and it was pioneered by Tutukov & Yungelson (1981) followed by the number of other studies (e.g., Iben & Tutukov 1984; Tornambe & Matteucci 1987; Jorgensen et al. 1997; Yungelson & Livio 2000; Han & Podsiadlowski 2004; Fedorova, Tutukov & Yungelson 2004). There are still many open problems in the field. As long as it is accepted that SN Ia are caused by the disruption of a white dwarf, the specific physical conditions leading to the explosion are widely discussed. Some important issues concern the white dwarf mass at which disruption followed by a SN can take place, accumulation rates on the white dwarf accretors, the outcome of double white dwarf mergers (SN Ia versus accretion induced collapse to neutron star) or the recently discussed issue of effects of rotation on white dwarf fate. Also, formation rates of different proposed SN Ia progenitors are not well constrained. The fact is that we lack an understanding of several evolutionary processes involved in the specific formation scenarios (e.g., common envelope phase). We refer the reader to several reviews for a de-

tailed discussion on an open issue of SN Ia progenitors (e.g., Branch et al. 1995; Renzini 1996; Livio 2000).

We consider three basic scenarios for SN Ia progenitors: single degenerate scenario (SDS, Whelan & Iben 1973; Nomoto 1982), semi-detached double white dwarf binary (SWB, Solheim & Yungelson 2004) model and double degenerate scenario (DDS, Webbink 1984; Iben & Tutukov 1984). In the SDS scenario a white dwarf (WD) accumulates mass from a non-degenerate companion star. Nuclear reactions are ignited in a WD which has accreted a sufficient layer of material on its surface. At the time of ignition the WD can have a mass below the Chandrasekhar limit, or the accretion may push it over this limit, and the ignition takes place when the WD is already unstable. Binaries consisting of two WDs may lead, under favorable conditions, to two qualitatively different progenitor SN Ia models. Both models involve WD pairs which are close enough such that at some point in their evolution, the less-massive (larger) WD overflows its Roche lobe, initiating the mass transfer phase. The SWB scenario takes place if mass transfer is dynamically stable and the pair evolves through the AM CVn stage (e.g., Nelemans et al. 2001) and the system may produce SN Ia if (i) the accreting WD is pushed over the Chandrasekhar limit or (ii) the accreted material is ignited on the WD of sub-Chandrasekhar mass leading to the edge-on lit detonation. The DDS takes place when the mass transfer is dynamically unstable and the less massive WD is rapidly accreted onto the companion WD. If the total mass of the WDs exceeds the Chandrasekhar limit the accretor either goes through accretion induced collapse and forms a neutron star or explodes in SN Ia (see Livio 2000 for review). In this work we *assume* that DDS results in a SN Ia explosion, in order to assess the model viability based on the time delay observations. All of the above scenarios imply

an evolutionary time delay between formation of the binary on the zero age main sequence (ZAMS) and the SN Ia explosion.

The recent results of the Hubble Higher  $z$  Supernova Search yielded a number of detections with redshifts up to  $z = 1.6$ . This allowed experimental determination of the delay time between the formation of a star on the ZAMS and supernova explosion (Strolger et al. 2004). They used three trial functions describing the delay time distribution: exponential, wide Gaussian and narrow Gaussian. Using the exponential function to describe the delay leads to a lower limit of 2.2-2.6 Gyrs, while the Gaussian fits lead to a constraint on the delay in the range of 2.4-3.8 Gyrs, or 3.6-4.6 Gyrs depending on the assumed star formation rate. In a separate study Gal-Yam & Maoz (2004) constrained the delay time to be longer than 1.7 Gyr.

In this paper we concentrate on calculation of the evolutionary delay times for different SN Ia progenitors, and compare them with the observational estimates of Strolger et al. (2004).

## 2. MODEL DESCRIPTION

The detailed description of the **StarTrack** population synthesis code is presented in Belczynski et al. (2002; 2005, in preparation). In the following we give an overview of the calculation scheme and summarize the most important features of the code.

### 2.1. Standard model

Each model calculation is started with an instantaneous starburst in which  $10^6$  binaries are formed and then evolved through the next 15 Gyrs. The mass of the primary (the more massive component) is drawn from the IMF with a three-component slope ( $-1.3/-2.2/-2.7$  with the exponent changing at 0.5 and 1.0  $M_{\odot}$ ; Kroupa & Weidner 2003) within the range 0.8 – 20  $M_{\odot}$ . The secondary mass is taken within the 0.08 – 20  $M_{\odot}$  range through a flat mass ratio (secondary/primary) distribution. The distribution of orbital separations is taken to be flat in the logarithm ( $\sim 1/a$ ) and we assume a thermal eccentricity distribution (2e).

The evolutionary calculations for stars (binary components) are based on modified formulae of Hurley et al. (2000). The modifications, which are described in Belczynski et al. (2002) are not relevant for this study (e.g., black hole mass spectrum). For all our presented calculations we evolve stars with a solar metallicity ( $Z = 0.02$ ).

Orbits of binary systems are allowed to change due to a number of physical processes. The recent magnetic braking law of Ivanova & Taam (2003) is included, with the saturation for fastest spinning stars. For tidal interactions we use the Hut (1981) equations but we increase the efficiency of tidal forces by an order of magnitude to recover the cutoff periods for several open clusters (Mathieu et al. 1992). We use Peters (1964) equations to include orbital decay due to the emission of gravitational radiation (GR). We also calculate the orbital expansion due to wind mass loss from binary components (Jeans mode mass loss). The wind mass loss rates are taken from Hurley et al. (2000), but extended to include winds for low- and intermediate-mass main sequence stars (Nieuwenhuijzen & de Jager 1990).

The **StarTrack** Roche lobe overflow (RLOF) treatment involves the detailed calculation of the mass transfer rates based on radius-mass exponents calculated both for the donor stars and their Roche lobes. The results of our calculations have been compared to a set of published detailed RLOF sequences (Wellstein, Langer & Braun 2001; Tauris & Savonije 1999; Dewi & Pols 2003) as well as to calculations obtained with an updated stellar evolution code (Ivanova et al. 2003). Our approach to the mass transfer calculations allows for the possibility of (i) conservative versus non-conservative RLOF episodes (ii) thermally driven RLOF versus nuclear/magnetic braking/gravitational radiation losses driven RLOF and (iii) a separation of systems as persistent or transient, depending on whether the donor RLOF mass transfer rate lies below the critical rate for instability to develop in the accretion disk (adopted from Dubus et al. 1999 or Menou, Perna & Hernquist 2002 for different compositions of transferred material).

For WD, neutron star (NS) and black hole (BH) accretors during dynamically stable RLOF phases the accretion is limited to Eddington critical rate with the rest of the transferred material lost from the system with the specific angular momentum of the accretor. For all the other accretors, we assume that only half of the transferred material is accreted (Meurs & van den Heuvel 1989) and the rest is lost with the specific binary angular momentum (Podsiadlowski, Joss & Hsu 1992).

### 2.2. Common Envelope Phases

*Standard Energy Balance Prescription* If dynamical instability is encountered the binary may enter a common envelope (CE) phase. We use the standard energy equations (Webbink 1984) to calculate the outcome of the CE phase

$$\alpha_{ce} \left( \frac{GM_{don}^f M_{acc}}{2A_f} - \frac{GM_{don}^i M_{acc}}{2A_i} \right) = \frac{GM_{don}^i M_{don,env}}{\lambda R_{don,rl}} \quad (1)$$

where,  $M_{don}$  is the mass of the donor,  $M_{acc}$  is the mass of the accretor,  $M_{don,env}$  is the mass of the donor's envelope,  $R_{don,rl}$  is the Roche lobe radius of the donor, and the indices  $i, f$  denote the initial and final values, respectively. Parameter  $\lambda$  describes the central concentration of the giant (de Kool 1990; Dewi & Tauris 2000). The right hand side of equation 1 expresses the binding energy of the donor's envelope, the left hand side represents the difference between the final and initial orbital energy, and  $\alpha_{ce}$  is the CE efficiency with which orbital energy is used to unbind the stellar envelope. If the calculated final binary orbit is too small to accommodate the two stars then a merger occurs. In our calculations, we combine  $\alpha_{ce}$  and  $\lambda$  into one CE parameter, and for our standard model, we assume that  $\alpha_{ce} \times \lambda = 1.0$ . If a compact object spirals in the common envelope it may accrete significant amounts of material because of hyper-critical accretion (Blondin 1986; Chevalier 1993; Brown 1995). We have incorporated the numerical scheme to include the effects of hyper-critical accretion on NSs and BHs in our standard CE prescription (for details see Belczynski et al. 2002).

*Alternative Angular Momentum Prescription* In addition to the standard prescription for the common enve-

lope evolution based on comparing the binding and orbital energies (Webbink 1984) we investigate the alternative approach (Nelemans & Tout 2005), based on the non-conservative mass transfer analysis by Paczynski & Ziolkowski (1967), with the assumption that the mass loss reduces the angular momentum in a linear way. This leads to reduction of the orbital separation

$$\frac{A_f}{A_i} = \left(1 - \gamma \frac{M_{\text{don,env}}}{M_{\text{tot}}^i}\right) \frac{M_{\text{tot}}^f}{M_{\text{tot}}^i} \left(\frac{M_{\text{don}}^i M_{\text{acc}}^i}{M_{\text{don}}^f M_{\text{acc}}^f}\right)^2 \quad (2)$$

where  $M_{\text{don,env}}$  is the mass of the lost envelope,  $M_{\text{tot}}^i$ ,  $M_{\text{tot}}^f$  are the total masses of the system before and after CE, and  $\gamma$  is a scaling factor. We use  $\gamma = 1.5$  following Nelemans & Tout (2005).

### 2.3. Mass Accumulation on White Dwarfs

In the following we describe mass accumulation on white dwarf accretors during dynamically stable RLOF phases. If mass transfer in a binary system containing a white dwarf and a non-degenerate companion is dynamically unstable, the system goes through a common envelope phase and we assume that the white dwarf does not accrete any matter. If dynamical instability is encountered for a binary with two white dwarfs we assume a merger. If the total mass of the two merging WDs is higher than  $1.4 M_{\odot}$  we assume a SN Ia explosion, independent of what type of WDs are merging. We comment on relaxing that assumption in the last section.

Accretion onto WDs may lead to a number of important phenomena, like nova or Type Ia SN explosions or even to an accretion induced collapse (AIC) of WD to a NS. In contrast to previous population synthesis studies, we incorporate the most recent results to estimate the accumulation efficiencies on WDs, which is crucial for the formation of SN Ia progenitors. In particular we consider accretion of matter of various compositions onto different white dwarf types. We also include the possibility that neutron star formation can occur via an AIC of a massive ONeMg white dwarf (Belczynski & Taam 2004a). The effect of an optically thick wind from the white dwarf surface, which can stabilize the mass transfer in the system at high mass transfer rates is taken into account (see Kato & Hachisu 1994; Hachisu, Kato, & Nomoto 1996, 1999). The accumulation rate of hydrogen-rich and helium-rich matter is taken from Hachisu et al. (1999) and Kato & Hachisu (1999) respectively (see also Ivanova & Taam 2004). For the direct accretion of helium or carbon/oxygen matter onto the ONeMg white dwarfs we make use of the work of Kawai, Saio & Nomoto (1987) in determining the evolution of the accreting white dwarf.

In the last few years several groups have initiated calculations of the effects of white dwarf rotation and spin-up due to the accretion (e.g., Piersanti et al. 2003; Uenishi, Nomoto & Hachisu 2003; Saio & Nomoto 2004; Yoon & Langer 2005). Some interesting results (obtained with 1- or 2-D simulations) were presented, e.g. the possibility of WD reaching super-Chandrasekhar mass, the possibly easier mass accumulation for SDS progenitors or avoidance of SN explosion through edge-on lit detonation at sub-Chandrasekhar mass. These results are not yet incorporated into our model, but they may have important consequences on progenitor models if they are confirmed.

*Accretion onto Helium white dwarf.* If the mass transfer rate  $\dot{M}_{\text{don}}$  from the H-rich donor is smaller than some critical value  $\dot{M}_{\text{crit1}}$ , there are strong nova explosions on the surface of the accreting WD, and no material is accumulated. The accumulation efficiency  $\eta_{\text{acu}} = 0.0$ , i.e. the entire transferred material is lost from the binary. If the  $\dot{M}_{\text{don}} > \dot{M}_{\text{crit1}}$  then the material piles up on the WD and leads to an inspiral. For giant-like donors we evolve the system through CE to see if the system survives; for all other donors we call it a merger and halt binary evolution. The critical transfer rate is calculated from:

$$\dot{M}_{\text{crit1}} = l_0 M_{\text{acc}}^{\lambda} (X * Q)^{-1} M_{\odot} \text{ yr}^{-1} \quad (3)$$

where,  $Q = 6 \times 10^{18} \text{ erg g}^{-1}$  is an energy yield of Hydrogen burning,  $X$  is the Hydrogen content of accreted material, and  $l_0$  and  $\lambda$  are coefficients. For Population I stars (metallicity  $Z > 0.01$ ) the values are  $X = 0.7$ ,  $l_0 = 1995262.3$ ,  $\lambda = 8$ , while for Population II stars ( $Z \leq 0.01$ ) we get  $X = 0.8$ ,  $l_0 = 31622.8$ ,  $\lambda = 5$  (Ritter 1999, see his eq. 10,12 and Table 2).

If the mass transfer rate from the He-rich donor is higher than  $\dot{M}_{\text{crit2}} = 2 \times 10^{-8} M_{\odot} \text{ yr}^{-1}$  all the material is accumulated ( $\eta_{\text{acu}} = 1.0$ ) until the accreted layer of material ignites in a helium shell flash at which point degeneracy is broken and a main sequence helium star is formed. Following the calculations of Saio & Nomoto (1998) we estimate the maximum mass of the accreted shell at which flash occurs:

$$\Delta M = \begin{cases} -7.8 \times 10^4 \dot{M} + 0.13 & \dot{M} < 1.64 \times 10^{-6} \\ 0(\text{instantaneous flash}) & \dot{M} \geq 1.64 \times 10^{-6} \end{cases} \quad (4)$$

where  $\dot{M}$  is expressed in  $M_{\odot} \text{ yr}^{-1}$ .

The newly formed helium star may overfill its Roche lobe, in which case either a single helium star is formed (He WD companion), a helium contact binary is formed (helium main sequence companion) or the system goes through CE evolution (evolved helium star companion).

For the lower than  $\dot{M}_{\text{crit2}}$  transfer rates, accumulation is also fully efficient ( $\eta_{\text{acu}} = 1.0$ ). However, the SN Ia occurs at the sub-Chandrasekhar mass:

$$M_{\text{SNIa}} = -400 \dot{M}_{\text{don}} + 1.34 M_{\odot}, \quad (5)$$

where  $\dot{M}_{\text{don}}$  is expressed in  $M_{\odot} \text{ yr}^{-1}$ . For mass transfer rates close to  $\dot{M}_{\text{crit2}}$ , the above extrapolations from the results of Hashimoto et al. (1986) yield masses smaller than the current mass of the accretor, and we assume instantaneous SN Ia explosion. We do not consider the accumulation of heavier elements since they could only originate from more massive WDs (e.g., CO or ONeMg WDs), which would have smaller radii and could not be donors to lighter He WDs.

*Accretion onto Carbon/Oxygen white dwarf.* We adopt the prescription from Ivanova & Taam (2004). In the case of H-rich donors for the mass transfer rates lower than  $10^{-11} M_{\odot} \text{ yr}^{-1}$  there are strong nova explosions and no material is accumulated ( $\eta_{\text{acu}} = 0.0$ ). In the range  $10^{-6} < \dot{M}_{\text{don}} < 10^{-11} M_{\odot} \text{ yr}^{-1}$  we interpolate for  $\eta_{\text{acu}}$  from Prialnik & Kovetz (1995, see their Table 1). For the

rates higher than  $10^{-6} M_{\odot} \text{ yr}^{-1}$  all transferred material burns into helium ( $\eta_{\text{acu}} = 1.0$ ). Additionally we account for the effects of strong optically thick winds (Hachisu et al. 1999), which blow away any material transferred over the critical rate

$$\dot{M}_{\text{crit}3} = 0.7510^{-6}(M_{\text{acc}} - 0.4) M_{\odot} \text{ yr}^{-1}. \quad (6)$$

This corresponds to  $\eta_{\text{acu}} = \dot{M}_{\text{crit}3}/\dot{M}_{\text{don}}$  for  $\dot{M}_{\text{don}} \geq \dot{M}_{\text{crit}3}$ . The accretor is allowed to increase mass up to  $1.4 M_{\odot}$ , and then explodes in a Chandrasekhar mass SN Ia. In the case of He-rich donors, if the mass transfer rate is higher than  $1.259 \times 10^{-6} M_{\odot} \text{ yr}^{-1}$  helium burning is stable and contributes to the accretor mass ( $\eta_{\text{acu}} = 1.0$ ). For the rates in the range  $5 \times 10^{-8} < \dot{M}_{\text{don}} < 1.259 \times 10^{-6} M_{\odot} \text{ yr}^{-1}$  accumulation is calculated from

$$\eta_{\text{acu}} = -0.175(\lg(\dot{M}_{\text{don}}) + 5.35)^2 + 1.05 \quad (7)$$

and represents the amount of material that is left on the surface of the accreting WD after the helium shell flash cycle (Kato & Hachisu 1999). The mass of the CO WD accretor is allowed to increase up to  $1.4 M_{\odot}$ , and then a Chandrasekhar mass SN Ia takes place in the two above He-rich accretion regimes. If mass transfer rates drops below  $5 \times 10^{-8} M_{\odot} \text{ yr}^{-1}$ , the helium accumulates on top of the CO WD and once the accumulated mass reaches  $0.1 M_{\odot}$  (Kato & Hachisu 1999), a detonation follows and ignites the CO core leading to the disruption of the accretor in a sub-Chandrasekhar mass SN Ia (e.g., Taam 1980; Garcia-Senz, Bravo & Woosley 1999). If the mass of the accreting WD has reached  $1.4 M_{\odot}$  before the accretion layer has reached  $0.1 M_{\odot}$  then the accretor explodes in a Chandrasekhar mass SN Ia. Carbon/Oxygen accumulation takes place without mass loss ( $\eta_{\text{acu}} = 1.0$ ) and leads to SN Ia if Chandrasekhar mass is reached.

*Accretion onto Oxygen/Neon/Magnesium white dwarf.* Accumulation onto ONeMg WDs is treated the same way as for CO WD accretors. The only difference arises when an accretor reaches Chandrasekhar mass. In the case of ONeMg WD this leads to an accretion induced collapse and neutron star formation, and binary evolution continues (see Belczynski & Taam 2004a; Belczynski & Taam 2004b).

### 3. RESULTS

#### 3.1. Typical evolution leading to SN Ia

The following examples of evolution leading to the formation of SN Ia progenitors in three different scenarios were calculated within our standard evolutionary model (see § 2.1).

*DDS Example.* The evolution starts with two intermediate-mass main sequence stars ( $M_1 = 6.0, M_2 = 4.5 M_{\odot}$ ) on a rather small ( $a \sim 200 R_{\odot}$ ) and eccentric orbit ( $e \sim 0.7$ ). First RLOF begins at  $\sim 70$  Myrs right after the primary evolves off the main sequence and is crossing the Hertzsprung Gap. The orbit has been already circularized ( $a \sim 60 R_{\odot}$ ). The ensuing MT is dynamically stable but proceeds on the thermal timescale of the donor and is characterized by a high transfer rate ( $\sim 3 \times 10^{-4} M_{\odot} \text{ yr}^{-1}$ ). After the rapid evolution through the Gap, the donor starts climbing the red giant branch,

where mass transfer continues but at slower rate driven by the nuclear evolution of donor ( $\sim 10^{-7} M_{\odot} \text{ yr}^{-1}$ ). Mass transfer stops when most of the donor envelope is exhausted. By this point the system has changed significantly; the primary becomes the less massive component ( $M_1 = 1.0 M_{\odot}$ ), the secondary is rejuvenated ( $M_1 = 7.0 M_{\odot}$ ) by accreted material, while the orbit has expanded ( $a \sim 380 R_{\odot}$ ) after mass ratio reversal. The rest of the primary envelope is lost in a stellar wind during core Helium burning and the primary becomes a low-mass naked helium star. The primary keeps evolving and at later stages expands and initiates the second RLOF (88 Myrs since ZAMS) which ends up in the formation of a CO WD ( $M_1 = 0.9 M_{\odot}$ ) when the primary is stripped this time of its helium-rich envelope. Then the secondary evolves off the main sequence and after 93 Myrs since ZAMS fills its Roche lobe while on the red giant branch. This leads to CE phase and a helium star ( $M_1 = 1.4 M_{\odot}$ ) is formed, this time out of the secondary, while the orbit shrinks significantly ( $a \sim 3 R_{\odot}$ ). The secondary evolves and eventually starts another RLOF, which stops after about 10 Myrs. The primary CO WD becomes quite massive ( $M_1 = 1.1$ ) due to accretion while the secondary loses most of its helium-rich envelope and becomes a CO WD ( $M_2 = 0.8 M_{\odot}$ ). This is the second mass ratio reversal in the system; the primary once again is the more massive binary component. A double CO WD binary, with total mass exceeding Chandrasekhar mass ( $M_1 + M_2 = 1.9 M_{\odot}$ ), is formed on a tight orbit ( $a = 2.7 R_{\odot}$ ) after about 100 Myrs since binary formation. The following orbital decay takes  $\sim 5$  Gyrs leading to the merger of two WDs and a possible SN Ia explosion.

*SWB Example.* The evolution starts with two relatively low-mass main sequence stars ( $M_1 = 1.7, M_2 = 1.5 M_{\odot}$ ) on a wide ( $a \sim 1000 R_{\odot}$ ) and highly eccentric orbit ( $e \sim 0.9$ ). After about 2 Gyrs the primary star evolves off the main sequence and shortly begins climbing up the red giant branch. The orbit circularizes and in the process the system becomes tighter ( $a \sim 200 R_{\odot}$ ). Eventually the primary overfills its Roche lobe, leading to a first CE phase. The primary loses its entire envelope and becomes a He WD ( $M_1 = 0.4 M_{\odot}$ ), and the orbit contracts farther ( $a \sim 10 R_{\odot}$ ). The secondary follows the same path as the primary – it evolves off the main sequence (in 3 Gyrs since ZAMS), becomes a red giant, overfills its Roche lobe and forms a second He WD ( $M_2 = 0.2 M_{\odot}$ ) in a second CE event (orbit contracts to  $a \sim 0.08 R_{\odot}$ ). The most recently formed (and lower mass) WD must be close to filling its Roche lobe so the gravitational radiation and associated orbital decay brings the system to contact within a Hubble time. At first RLOF proceeds with a high (but dynamically stable) mass transfer rate ( $\sim 10^{-6} M_{\odot} \text{ yr}^{-1}$ ) but soon it drops down ( $\sim 10^{-8} M_{\odot} \text{ yr}^{-1}$ ) to the regime when the material can accumulate on the primary leading to the final explosion and disruption of the primary WD. At the moment of explosion, the primary WD has accreted about  $0.1 M_{\odot}$  and exploded at sub-Chandrasekhar mass ( $M_1 = 0.5 M_{\odot}$ ).

*SDS Example.* The evolution starts with two intermediate-mass main sequence stars ( $M_1 = 4.5, M_2 = 3.4 M_{\odot}$ ) on a very wide ( $a \sim 4400 R_{\odot}$ ) and highly eccentric orbit ( $e \sim 0.8$ ). The primary evolves all the way to

the late asymptotic giant branch before filling its Roche lobe. The orbit circularizes before contact is reached ( $a \sim 1500 R_\odot$ ). The RLOF leads to first CE phase, orbital contraction ( $a \sim 60 R_\odot$ ) and formation of a CO WD ( $M_1 = 0.9 M_\odot$ ) at  $\sim 160$  Myrs since ZAMS. The secondary takes another  $\sim 100$  Myrs to evolve off the main sequence. This time due to the smaller orbit size, the Roche lobe is encountered when the donor (secondary) is on the red giant branch. The second CE phase ensues, leading to further orbital contraction ( $a \sim 0.5 R_\odot$ ), and the exposed core of the secondary (which is non-degenerate) forms a naked helium main sequence star ( $M_2 = 0.5 M_\odot$ ). The orbit slowly decays owing to the tidal spin up of the secondary, and finally after synchronization is reached the third RLOF is encountered when the Helium star exceeds its Roche lobe ( $a \sim 0.4 R_\odot$ ) 275 Myrs since ZAMS. This time mass transfer is dynamically stable ( $\sim 10^{-8} M_\odot \text{ yr}^{-1}$ ), and helium-rich material is transferred and accumulated on the CO WD primary. After about 5 Myrs of accretion the layer accumulated on the WD explodes leading to primary ( $M_1 = 1.0 M_\odot$ ) disruption in sub-Chandrasekhar SN Ia.

### 3.2. Delay Times

The delay times can be contributed to three major processes: (i) evolution of stars to form two WDs (DDS, SWB), or to form a WD in RLOF system with non-degenerate companion (SDS); (ii) orbital decay (GR) to bring a system to contact after formation of WD-WD binary (DDS, SWB); (iii) accumulation of sufficient amount of material on the WD surface to initiate SN Ia explosion (SWB, SDS).

The first contribution (i) is set by the mass of the secondary star, since the evolution time depends very strongly on initial mass and is longer for lower mass stars. These times are on average: 0.1 Gyr (DDS, secondaries  $\sim 3-8 M_\odot$ ), 0.4–12 Gyr (SWB, secondaries  $\sim 1-3 M_\odot$ ), and  $\sim 0.5$  Gyr (SDS, secondaries  $\sim 2-4 M_\odot$ ).

The second contribution (ii) is set by the GR timescale for a given system, which depends very strongly on the orbital separation of two WDs. The orbital separation in turn is basically set by the CE efficiency. The majority of SN Ia progenitors evolve through one or two CE phases. The only significant changes to orbital separation are encountered during these phases (orbital contractions by factors of 10-100). Therefore, this part of delay is set by the CE efficiency and it may vary over a wide range, basically from zero to a Hubble time.

The third contribution (iii) is set by the accumulation efficiencies described in §2.3. For a given type of system, we expect a specific mass transfer rate and a corresponding accumulation rate which sets the time of SN Ia explosion. The efficient accumulation happens only in a given mass transfer range, and this part of the delay is easily predicted. On average these times are around one Myr for SWB and several Myrs for SDS progenitors.

Summarizing, we see that for DDS progenitors the delay time is set basically by the GR orbital decay, for SWB systems both GR and evolutionary effects play an important role, while for SDS systems the major contribution comes from evolutionary times. In general, the time needed for the accumulation on the WD surface does not play a significant role.

### 3.3. Statistics

It may be inferred from the evolutionary histories of SN Ia progenitors that the CE efficiency is a major factor influencing the SN Ia delay times. Almost all progenitors evolve through at least one CE phase. The CE phase basically sets the timescale for GR orbital decay of DDS and SWB systems. For SDS systems the CE orbit contraction sets the initial conditions for a RLOF phase with corresponding mass transfer rate, which if falls into a specific regime, may lead a system to SN Ia explosion. Unfortunately, the CE phase is not well constrained, therefore we will perform the calculation of the delay times with different CE efficiencies and treatments.

*Standard Model.* It is found that within the SDS, exploding WDs are: mainly CO WDs (82%) and a smaller number of He WDs (11%), ONeMg WDs (4%) and hybrid (CO core/He envelope) WDs (3%) with various types of donors. In the SWB progenitor group the systems are: double He WD binaries (77%), CO WD – hybrid WD systems (21%), with the rest being different combinations of He, CO, hybrid and ONeMg WDs. Within the DDS class we find that most of the SN Ia progenitors are CO-CO WDs (88%), and the rest are binaries hosting one or two ONeMg WDs (12%). The relative numbers of potential SN Ia progenitors are: 13% (SDS), 49% (SWB) and 38% (DDS). We note that DDS progenitors constitute the most uniform group among three progenitor classes.

*Alternative CE Models.* In the models with decreased CE efficiency we note a decrease in the number of potential SN Ia progenitors by factors of 3 and 6, corresponding to models with  $\alpha\lambda = 0.3$  and  $\gamma = 1.5$ , respectively. This is expected since many potential progenitors evolve through a CE phase, and will not survive this phase if the efficiency is smaller than in our standard model. However, as argued by Nelemans & Tout (2005), the decreased CE efficiency may be needed to explain the observed population of double WDs. We also note that for these models DDS is more efficient in producing SN Ia progenitors (70%) as compared to the combined SDS and SWB classes (30%).

In all models DDS progenitors (by definition) explode at Chandrasekhar mass. It is found in all calculations that progenitors in the SWB class explode at sub-Chandrasekhar mass. For the SDS scenario in the standard model and the model with  $\alpha\lambda = 0.3$  it is found that only a small fraction of WDs (6%) explode at Chandrasekhar mass with the majority of systems (94%) exploding at sub-Chandrasekhar mass. Only for the model with the alternative CE prescription with  $\gamma = 1.5$  will the fraction of SDS progenitors exploding at Chandrasekhar mass become significant (37%).

### 3.4. Delay time distributions

For each scenario leading to a potential formation of a SN Ia we note the time  $T$  between the formation of the binary system on ZAMS and the explosion. This gives us a distribution of time delays. Ideally we would wish to compare such a distribution with the observed one. However, observations provide us with one characteristic property of the delay distribution, i.e. the typical delay time. Thus for each distribution we obtain, we calculate two timescales: the mean  $t_{\text{av}}$  and the median  $t_{50}$  and use them for comparison. In order to better characterize the distributions

we also calculate the 25% and 75% quantiles of the distribution:  $t_{25}$ , and  $t_{75}$ . We assume that the characteristic timescale of a given model lies somewhere between  $t_{av}$  and  $t_{50}$ . We list these characteristic times in Table 1.

We present the distribution of delay times within the standard model in the left panel of Figure 1. In the case of SDS the distribution peaks between 0.4 and 0.8 Gyr, and has a weak tail extending to later times. The typical systems in this group consist of a CO WD accreting either from a He main sequence star or hybrid WD, originating from binaries with intermediate mass components ( $M_{zams} \sim 2 - 4 M_{\odot}$ ).

In the case of the SWB the distribution is bimodal. The long delay time peak ( $\sim 10$  Gyrs) corresponds to a majority of systems in SWB class: He WD - He WD binaries (77%, see §3.3), while the short delay time peak ( $\sim 0.5$  Gyrs) corresponds to CO WD - hybrid WD systems (21%). The double He WDs descend from the low mass stars (secondaries  $\sim 1 M_{\odot}$ ) and therefore the long evolutionary time adds up to the overall delay time (see §3.2). The CO WD - hybrid WD progenitors descend from more massive stars (secondaries  $\sim 3 M_{\odot}$ ) and the evolutionary time does not contribute significantly for the overall delay time. The truncation at long times is artificial, as we are not considering the evolution beyond the Hubble time.

The distribution of lifetimes in the case of DDS is nearly flat in  $TdN/dT$ , and stretches from about 0.2 Gyr to the Hubble time. This distribution is similar to the one obtained by e.g. Jorgensen et al. (1997) and Yungelson & Livio (2000).

In the top rows of Table 1 we show the characteristic times for the standard model. In the case of the SDS both the average and the mean delay time are below 1 Gyr. For the SWB model the typical timescales are dominated by the late end of the distribution and are above 7 Gyrs. In the case of the DDS the average and the median delay time are in the 1.8-3.2 Gyr range. Comparison of these times with the delay times found by Strolger et al. (2004) argues strongly for the DDS as progenitors of SN Ia.

Table 1 also contains the characteristic delay times for the two alternative models we have considered, and we present these distributions in the middle and right panel of Figure 1. In the model with  $\alpha\lambda = 0.3$  the situation is similar to the standard model described above. The typical delay times in the SDS case of 0.7-1.8 Gyr are smaller than the Strolger et al. (2004) result, while in the SWB case these times are much higher. On the other hand the delay times in the DDS case of 2.9-4.3 Gyr are again in agreement with Strolger et al. (2004).

The results of the calculations with the alternative description of the CE phase ( $\gamma = 1.5$ ) are shown in the right panel of Figure 1 and the bottom rows of Table 1. In this case the characteristic times in each scenario (SDS, SWB, DDS) are consistent with the range 2-4 Gyrs of Strolger et al. (2004). We note however that in the case of SWB the delay time distribution is bimodal and has a minimum just in the range of 2-7 Gyrs. We note that the SDS model can be tuned with a proper treatment of the CE phase to agree with the Strolger et al. (2004) timescale. On the other hand the delay time distribution in the DDS model is consistent with the 2-4 Gyrs range irrespective of the CE phase description.

#### 4. DISCUSSION AND SUMMARY

We have calculated the distributions of delay times between a burst of star formation and supernovae type Ia explosions with the use of the `StarTrack` population synthesis code. We have considered three different models of the CE evolution, characterized by two values of  $\alpha\lambda$  and  $\gamma$ . We find that the distribution of delay times in the DDS scenario is approximately flat in  $TdN/dT$ , while for the case of SDS and SWB models it can be bimodal. We characterized the shape of these distributions by the average and the median, and compare these times with the typical delay range of 2-4 Gyr found by Strolger et al. (2004). The characteristic values describing the distribution of delay times in the DDS are consistent with the 2-4 Gyr value in each of the three evolutionary models. In the case of SDS we find that one can tune the CE description such that the average and median of the delay time distribution fits in the 2-4 Gyrs range. The typical delay times in the SWB SN Ia progenitor class are above 7 Gyr except for the  $\gamma = 1.5$  model. However, in this case the delay time distribution is bimodal and has a minimum for the values corresponding to the average or the median.

The estimated long delay times were noted to favor the DDS over SDS SN Ia progenitor model by Gal-Yam & Maoz (2004), who used Yungelson & Livio (2000) results showing rather long delay times for the DDS model, as opposed to shorter delay times for SDS progenitors. On the contrary, Dahlen et al. (2004) noted that the long delay times give support to SDS SN Ia progenitor model, but the statement was not backed up with any arguments or calculations. Our results show that in general DDS delay times are longer than for SDS progenitors (see Table 1). However, we find that for the model with the alternative CE treatment the SDS delay times are as long as DDS times, and are consistent with observations.

It was also noted (e.g., Hofflich et al. 1996; Nugent et al. 1997) that observed properties of SN Ia favor explosion of WD at Chandrasekhar mass, while the sub-Chandrasekhar mass models do not explain even subluminal, red SN Ia. As described in §3.3 only for the DDS scenario do we expect Chandrasekhar mass SN Ia in all models. All SWB systems explode at sub-Chandrasekhar mass. The majority of SDS systems explode also at sub-Chandrasekhar mass (standard and  $\alpha\lambda = 0.3$  models) and only for the model with the alternative CE treatment (with  $\gamma = 1.5$ ) it is found that a significant fraction of SDS progenitors explode at Chandrasekhar mass. Therefore, the mass of an exploding WD points toward the DDS scenario, with the possibility that the SDS scenario may provide possible Chandrasekhar mass progenitors in the model with  $\gamma = 1.5$  CE treatment. The SWB scenario is basically excluded as the potential SN Ia progenitor.

We conclude that the DDS is the preferred progenitor type of SN Ia based on the comparison of the delay distribution times with the observational analysis by Strolger et al. (2004). Our calculations show that within the DDS scenario the SN Ia progenitor population consists mainly of CO-CO WD binaries, hence the uniform properties of SN Ia are a natural result. Finally, it is now known that such systems exist since Napiwotzki et al. (2004) found a double degenerate system with a total mass exceeding the Chandrasekhar mass and a 4 Gyr merger time. How-

ever, we note that the recent calculations (e.g., Timmes, Woosley & Taam 1994; Saio & Nomoto 1998) may indicate that massive WD mergers would lead to accretion induced collapse rather than to SN Ia. If this is the case, then our results for SDS SN Ia progenitors could be shown to be consistent with the delay time observations, provided that the CE efficiency is rather low. There may be also some observational evidence supporting SDS progenitor model. Ruiz-Lapuente et al. (2004) have searched for possible companions to Tycho Brahe's 1572 supernova, and concluded that the most probable companion was a G star. Also, Hamuy et al. (2003) observed SN 2002ic and reported strong hydrogen emission from circumstellar material, and interpreted it in context of the companion star being an asymptotic giant star which has created a bubble of H-rich material around the progenitor through stellar wind mass loss. However, this interpretation was countered by Livio & Riess (2003) who presented the picture in which a DDS progenitor can also account for the H-rich circumstellar material. The H-rich gas would originate from a common envelope phase which would result in the merging of a white dwarf and the degenerate core of the companion followed by a supernova. Also the results indicating that massive WD mergers lead to an accretion

induced collapse, may now be opposed with the calculations including rapid WD rotation (e.g., Piersanti et al. 2003). The rotation stabilizes the accretion and the massive merger may actually lead to SN Ia, lending support to the DDS scenario. It is also possible that SN Ia originate from various progenitor classes, and further observations are needed to resolve the issue and guide theoretical studies.

The shape of the delay time distribution is different for the three progenitor scenarios (see Fig 1). The different shapes could be tested against observations in order to get better constraints on progenitor classes, e.g.  $dN/dT \propto T^{-1}$  for DDS. We note that in order to assess the viability of the SDS or SWB one should attempt to model the supernova survey results with a bimodal distribution of delay times.

We would like to thank Tom Harrison and Ron Taam for comments on this project and anonymous referee for very detailed and useful report. We acknowledge support from KBN through grant PBZ-KBN-054/P03/2001. TB wishes to thank for the hospitality of the NMSU Department of Astronomy, while KB and TB acknowledge local support from Pike Lilley (Alamo).

#### REFERENCES

- Belczynski, K., Kalogera, V., & Bulik, T. 2002, *ApJ*, 572, 407  
 Belczynski, K., & Taam, R. E. 2004a, *ApJ*, 603, 690  
 Belczynski, K., & Taam, R. E. 2004b, *ApJ*, 616, 1159  
 Blondin, J.M. 1986, *ApJ*, 308, 755  
 Branch, D., Livio, M., Yungelson, L.R., Boffi, F.R., & Baron, E. 1995, *PASP*, 107, 1019  
 Brown, G.E. 1995, *ApJ*, 440, 270  
 Chevalier, R.A. 1993, *ApJ*, 411, L33  
 Dahlen, T., et al. 2004, *ApJ*, 613, 189  
 Dewi, J.D.M., & Pols, O.R. 2003, *MNRAS*, 344, 629  
 Dewi, J.D.M., & Tauris, T.M. 2000, *A&A*, 360, 1043  
 de Kool, M. 1990, *ApJ*, 358, 189  
 Dubus, G. et al. 1999, *MNRAS*, 303, 139  
 Fedorova, A. V., Tutukov, A. V., & Yungelson, L. R. 2004, *Astronomy Letters*, 30, 73  
 Gal-Yam, A., & Maoz, D. 2004, *MNRAS*, 347, 942  
 Garcia-Senz, D., Bravo, E., & Woosley, S.W. 1999, *A&A*, 349, 177  
 Hachisu, I., Kato, M., & Nomoto, K. 1996, *ApJ*, 470, L97  
 Hachisu, I., Kato, M., & Nomoto, K. 1999, *ApJ*, 522, 487  
 Hamuy, M., et al. 2003, *Nature*, 424, 651  
 Han, Z., & Podsiadlowski, P. 2004, *MNRAS*, 350, 1301  
 Hashimoto, M.A., Nomoto, K.I., Arai, K., & Kaminisi, K. 1986, *ApJ*, 307, 687  
 Hofflich, P., et al. 1996, *ApJ*, 472, L81  
 Hurley, J. R., Pols, O. R., & Tout, C. A. 2000, *MNRAS*, 315, 543  
 Hut, P. 1981, *A&A*, 99, 126  
 Iben, I., & Tutukov, A.V. 1984, *ApJS*, 54, 355  
 Ivanova, N., Belczynski, K., Kalogera, V., Rasio, F., & Taam, R. E. 2003, *ApJ*, 592, 475  
 Ivanova, N., & Taam, R. E. 2003, *ApJ*, 599, 516  
 Ivanova, N., & Taam, R. E. 2004, *ApJ*, 601, 1058  
 Jorgensen, H. E., Lipunov, V. M., Panchenko, I. E., Postnov, K. A., & Prokhorov, M. E. 1997, *ApJ*, 486, 110  
 Kato, M., & Hachisu, I. 1994, *ApJ*, 437, 802  
 Kato, M., & Hachisu, I. 1999, *ApJ*, 513, L41  
 Kawai, Y., Saio, H., & Nomoto, K. 1987, *ApJ*, 315, 229  
 Kroupa, P., & Weidner, C. 2003, *ApJ*, 598, 1076  
 Livio, M. 2000, *Type Ia Supernovae, Theory and Cosmology*. Edited by J. C. Niemeyer and J. W. Truran. Published by Cambridge University Press, 2000., p.33  
 Livio, M., & Riess, A.G. 2003, *ApJ*, 594, L93  
 Mathieu, R. D., Duquenooy, A., Latham, D. W., Mayor, M., Mermilliod, T., & Mazeh, J. C. 1992, *Proceedings of "Binaries as Tracers of Stellar Formation"*, ed. Duquenooy, A. & Mayor, M., Cambridge University Press, p.278  
 Menou, K., Perna, R., & Hernquist, L. 2002, *ApJ*, 564, L81  
 Meurs, E.J.A., & van den Heuvel, E.P.J. 1989, *A&A*, 226, 88  
 Napiwotzky, R. et al. 2004, *ASP Conf series* 318, 402  
 Nelemans, G., Portegies Zwart, S. F., Verbunt, F., & Yungelson, L. R. 2001, *A&A*, 368, 939  
 Nelemans, G., & Tout, C. A. 2005, *MNRAS*, 356, 753  
 Nieuwenhuijzen, H., & de Jager, C. 1990, *A&A*, 231, 134  
 Nomoto, K. 1982, *ApJ*, 253, 798  
 Nugent, P., Baron, E., Branch, D., Fisher, A., & Hauschildt, P.H. 1997, *ApJ*, 485, 812  
 Paczynski, B., & Ziolkowski, J. 1967, *Acta Astronomica*, 17, 7  
 Perlmutter, S., et al. 1999, *ApJ*, 517, 565  
 Peters, P. C. 1964, *Phys.Rev.*, 136, B1224  
 Piersanti, L., Gagliardi, S., Iben, I., & Tornambe, A. 2003, *ApJ*, 598, 1229  
 Podsiadlowski, P., Joss, P.C., & Hsu, J.J.L. 1992, *ApJ*, 391, 246  
 Prialnik, D., & Kovetz, A. 1995, *ApJ*, 445, 789  
 Renzini, A. 1996, *Supernovae and supernova remnants*. *Proceedings of the IAU Coll. 145*; Cambridge University Press; edited by R. McCray & Z. Wang, p.77  
 Riess, A. G., et al. 2001, *ApJ*, 560, 49  
 Ritter, H. 1999, *MNRAS*, 309, 360  
 Ruiz-Lapuente, P., et al. 2004, *Nature*, 431, 1069  
 Saio, H., & Nomoto, K. 1998, *ApJ*, 500, 388  
 Saio, H., & Nomoto, K. 2004, *ApJ*, 615, 444  
 Schmidt, B. P., et al. 1998, *ApJ*, 507, 46  
 Solheim, J.E., & Yungelson, L.R. 2004, *EUROWD 2004 - 14th European Workshop on White Dwarfs*, *ASP Conf. Series*, submitted (astro-ph/0411053)  
 Strolger, L., et al. 2004, *ApJ*, 613, 200  
 Taam, R.E. 1980, *ApJ*, 242, 719  
 Tauris, T.M., & Savonije, G.J. 1999, *A&A*, 350, 928  
 Tegmark, M., et al. 2004, *Phys. Rev. D*, 69, 103501  
 Timmes, F.X., Woosley, S.E., & Taam, R.E. 1994, *ApJ*, 420, 348  
 Tornambe, A., & Matteucci, F. 1987, *ApJ*, 318, L25  
 Tonry, J. L., et al. 2003, *ApJ*, 594, 1  
 Tutukov, A.V., & Yungelson, L. 1981, *Naychnye Informatsii Astron. Soveta*, 49, 3  
 Uenishi, T., Nomoto, K., & Hachisu, I. 2003, *ApJ*, 595, 1094  
 Wellstein, S., Langer, N., & Braun, H. 2001, *A&A*, 369, 939  
 Webbink, R. F. 1984, *ApJ*, 277, 355  
 Whelan, J., & Iben, I. 1973, *ApJ*, 186, 1007  
 Yoon, S.C., & Langer, N. 2005, *A&A*, submitted (astro-ph/0502133)  
 Yungelson, L. R., & Livio, M. 2000, *ApJ*, 528, 108

TABLE 1  
SN IA DELAY TIMES [GYR]

$\alpha\lambda = 1.0$	$t_{av}$	$t_{25}$	$t_{50}$	$t_{75}$
SDS	0.85	0.32	0.43	0.62
SWB	7.60	3.78	8.21	11.5
DDS	3.30	0.60	1.76	4.70
$\alpha\lambda = 0.3$				
SDS	1.89	0.12	0.73	3.10
SWB	10.5	10.6	12.6	13.8
DDS	4.39	0.65	2.92	7.57
$\gamma = 1.5$				
SDS	2.90	0.83	2.61	3.85
SWB	4.57	0.73	1.10	10.6
DDS	3.06	0.34	1.18	4.71



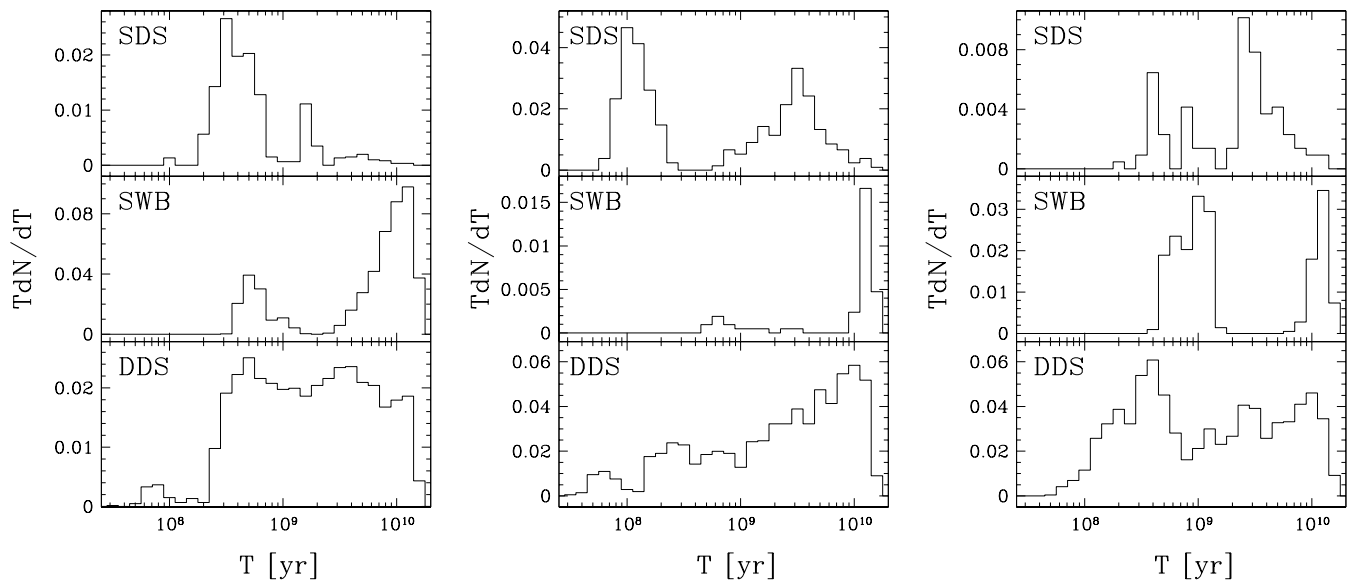


Fig. 1.— The distribution of SN Ia delay times since the burst of star formation. The left panel shows the results of our standard model calculation ( $\alpha\lambda = 1.0$ ), the middle panel corresponds to evolution with the decreased CE efficiency ( $\alpha\lambda = 0.3$ ), while in the right panel we present results for alternative CE description ( $\gamma = 1.5$ ). The three different classes of SN Ia progenitors are shown on each panel: single degenerate scenario (top), semi-detached double WD binaries (middle) and double degenerate scenario (bottom). The distributions are normalized to the sum of all SN Ia progenitors (SDS+SWB+DDS) in the model. The data are binned in the intervals with the width of 0.1 in  $\log(T/\text{yr})$ .